A Renewal Theory Based Analytical Model for Multi-Channel Random Access in IEEE 802.11ac/ax

Sami Khairy, *Student Member, IEEE*, Mengqi Han, *Student Member, IEEE*, Lin X. Cai, *Member, IEEE*, Yu Cheng, *Senior Member, IEEE*, and Zhu Han, *Fellow, IEEE*

Abstract—To support bandwidth-intensive services such as virtual reality video applications, next generation WLANs will allow users to transmit over multiple channels for high data rate transmissions. In this paper, an analytical model is developed to study the performance of the dynamic channel bonding in IEEE 802.11ac, and non-contiguous channel aggregation in IEEE 802.11ax, with coexisting legacy single channel users. By modeling the transmissions of single channel and multi-channel users with and without channel bonding as a two-level renewal process, the bonding probability of multi-channel users, along with the throughput of different users in each channel, are derived. Our analysis shows that multi-channel users can boost their throughput at the cost of degraded throughput of legacy users. Furthermore, it is shown that 802.11ax provides higher spectrum utilization compared to 802.11ac, while 802.11ac provides a friendlier coexistence with single channel users. Based on the analysis, a heuristic algorithm for primary channel selection is further proposed to maximize the throughput of multi-channel users. Extensive simulations using NS-3 validate the analysis and demonstrate the efficiency of the proposed channel selection algorithm.

Index Terms—Performance analysis, WLANs, multi-channel bonding, multi-channel aggregation, IEEE 802.11ac, IEEE 802.11ax, primary channel selection

1 Introduction

According to Cisco's data traffic forecast, video traffic will account for 78 percent of the world's data traffic by 2021 [1]. On-demand, 4 K Ultra High Definition (UHD) video streaming, which requires a bandwidth on the order of tens of megabits per second, is replacing cable and satellite TV nowadays. Virtual reality is likely another bandwidth hungry video application, which may become an integral part of the workplace and education system in the future. This poses new challenges for next generation Wireless Local Area Networks (WLANs), which are required to provide increased user capacity and throughput.

To keep up with such demands, a multi-channel Medium Access Control (MAC) protocol, known as the Dynamic Channel Bonding (DCB) was specified in IEEE 802.11ac to allow users to opportunistically bond multiple consecutive non-overlapping channels for high data rate transmissions over a wider bandwidth. Channel Aggregation (CA) is further proposed in the IEEE 802.11ax study group to remove the consecutive channel bonding restriction. In addition to physical layer techniques, such as high order modulation and multiple input multiple output (MIMO), these MAC enhancements have paved the way for Gigabit WLANs.

The performance of a conventional WLAN operating based on the Carrier Sensing Multiple Access with Collision Avoidance (CSMA/CA) based MAC, has been extensively studied in the literature [2], [3], [4], [5]. Analytical models developed for single channel WLANs, however, cannot be readily applied to multi-channel WLANs, because multi-channel random access involves different access technologies in different channels. Although the contiguous channel bonding and non-contiguous channel aggregation features of IEEE 802.11ac and IEEE 802.11ax, respectively, have great potential to improve the throughput of WLANs, there are only few research works that study their performance. The existing works on multi-channel WLANs are either based on experimental studies [6], simulations [7], or simplified analytical models with strong assumptions [8], [9]. To the best of our knowledge, there is no generic analytical work for distributed channel bonding or channel aggregation in multi-channel WLANs, characterizing different access technologies in different channels realistically and accurately. How to efficiently select the primary channel for multi-channel WLAN users to maximize their throughput, also remains an open research question. Thus motivated, we analyze multi-channel random access under general coexistence scenarios and different bonding schemes, considering the contention among multiple and single channel users, and further propose an algorithm to enable efficient multi-channel access in 802.11 WLANs.

In this paper, a generic analytical model is developed to study the performance of multi-channel WLANs adopting

- *S. Khairy, M. Han, L.X. Cai, and Y. Cheng are with the Department of Electrical and Computer Engineering, Illinois Institute of Technology, Chicago, IL 60616. E-mail: {skhairy, mhan9}@hawk.iit.edu, {lincai, cheng}@iit.edu.*
- *Z. Han is with the Department of Electrical and Computer Engineering, University of Houston, Houston, TX 77004, and the Department of Computer Science and Engineering, Kyung Hee University, Seoul, South Korea. E-mail: zhan2@uh.edu.*

Manuscript received 23 Sept. 2017; revised 22 Apr. 2018; accepted 13 July 2018. Date of publication 19 July 2018; date of current version 1 Apr. 2019. (Corresponding author: Sami Khairy.)
For information on obtaining reprints of this article, please send e-mail to: reprints@ieee.org, and reference the Digital Object Identifier below.
Digital Object Identifier no. 10.1109/TMC.2018.2857799

dynamic channel bonding protocols, including the restricted channel bonding specified in IEEE 802.11ac, a generalized form of it, which is referred to as the unrestricted contiguous channel bonding, and the non-contiguous channel aggregation proposed in IEEE 802.11ax. Specifically, we consider a realistic WLAN with coexisted multi-channel users and legacy single channel users. Applying a two-level renewal process based model, the channel access behaviors of multi-channel and single channel users are analyzed, and the interactions between different users are well characterized, including the possible collisions between multiple and single channel users, which have been ignored in other major research works. The channel bonding probability of multi-channel users, and the throughput of multiple and single channel users in each channel are derived under different channel bonding schemes. The impacts of primary channel selection are also shown, and based on the analysis, we further propose a heuristic algorithm for multi-channel users to select the best primary channel to maximize their throughput. Finally, we implement the various bonding schemes in an event driven simulation platform based on Network simulator 3 (NS-3), and conduct extensive simulations to validate the analytical model and demonstrate the efficiency of the proposed channel selection algorithm.

The remainder of this paper is organized as follows. The dynamic channel bonding MAC of IEEE 802.11ac, the generalized contiguous channel bonding MAC and the non-contiguous channel bonding MAC of IEEE 802.11ax are described in Section 2. A literature survey of related research work is presented in Section 3. An analytical framework is developed in Section 4 to analyze the performance of each bonding scheme. The optimal primary channel selection and the designed heuristic alogrithm are proposed in Section 5. The performance evaluation of the different bonding schemes and the efficiency of the proposed algorithm are presented in Section 6. Finally, our concluding remarks and future work are provided in Section 7.

2 Channel Bonding Protocols

2.1 IEEE 802.11n/ac Channel Bonding MAC

A distributed DCB MAC was proposed in IEEE 802.11n [10] and IEEE 802.11ac [11] to enable Gigabit WLANs and support high throughput multimedia applications. Basically, users can group two (in IEEE 802.11n) or more 20 MHz channels (in IEEE 802.11ac) into one channel with a larger bandwidth for higher data rate transmissions.

In this MAC, a user first selects a primary channel in which it operates according to the CSMA/CA based legacy Distributed Coordination Function (DCF) [2], [12], [13]. That is, a user can transmit only when the channel is sensed idle for a DIFS. If the channel is busy, a backoff counter is uniformly picked from $[0, CW_0]$, where CW_0 is the minimum contention window. The counter is decremented by 1 every idle slot and is frozen otherwise. Once frozen, the user persists to sense the channel, and resumes decrementing the counter when the channel is sensed idle for a DIFS again. When the counter reaches 0, the user transmits immediately. Contention window doubles after each unsuccessful transmission, until the maximum contention window CW_{max} is reached, and is reset to CW_0 after every successful transmission. In the meantime, the user also senses secondary channels, and bonds the largest contiguous subset of secondary channels that are sensed idle for a PIFS[1] before the user transmits in the primary channel. If the first secondary channel is busy, transmission proceeds on the primary channel solely. According to the IEEE 802.11ac standard, the number of contiguous basic channels which can be bonded for a transmission must be powers of two, i.e., $2, 4,$ and 8 (optional). If a collision occurs in any of the primary or secondary channels selected for transmission, transmission fails and the user will contend for a retransmission. Thus, in an 802.11n/ac based WLAN, users opportunistically access different numbers of channels using different technologies, i.e., DCF based channel access in the primary channel and simple sensing without backoff in secondary channels.

2.2 Unrestricted Contiguous Channel Bonding

In this paper, a generalized form of the 802.11ac DCB is also considered, which is referred to as the Unrestricted Contiguous Channel Bonding (UCCB). It is similar to the 802.11ac DCB scheme in the sense that users bond the largest contiguous subset of secondary channels, which are sensed idle for a PIFS before the user transmits in the primary channel. However, there is no limitation on the number of contiguous basic channels used for transmission, i.e., a user can bond $2, 3, 4, \ldots,$ up to 8 channels, whichever was idle. We show that this channelization scheme can achieve a better performance than the 802.11ac DCB, especially when some 20 MHz wide chunks are under-utilized, yet the bigger 40, 80 or 160 MHz wide chunks to which they belong are not totally under-utilized.

2.3 IEEE 802.11ax Channel Aggregation MAC

The high efficiency WLAN study group started working on a new IEEE 802.11 amendment in 2014, to further improve the spectrum efficiency and provide an increased system throughput in high dense WLANs [14]. IEEE 802.11ax, which is expected to be released in 2019 as an amendment to both IEEE 802.11n and IEEE 802.11ac, aims to achieve at least a fourfold increase in throughput, compared to IEEE 802.11ac [15]. The IEEE 802.11ax amendment is in its initial stages of development; however, non-contiguous channel bonding is being considered as a means to achieve this fourfold throughput increase. Non-contiguous channel bonding, or channel aggregation, provides a higher flexibility to leverage under-utilized secondary channels, by allowing users to bond any available secondary channel without any contiguity restriction. Although the granularity of non-contiguous channels is still unspecified, a primary 20 MHz channel will always be used for transmission [14]. Channel aggregation is possible in 802.11ax due to the introduction of OFDMA, which adds a new degree of freedom in spectrum access. It is likely that channel aggregation will be allowed for downlink transmissions to support multi-users. In this paper, we consider a basic implementation of OFDMA, in which each 20 MHz channel can be independently aggregated with the primary channel for a high data rate transmission over a wider bandwidth.

1. According to the IEEE 802.11ac standard, PIFS=SIFS+1$*$slot, while DIFS=SIFS+2$*$slots.

3 Related Work

The performance of a legacy single channel WLAN with a CSMA/CA based MAC, has been studied in a wide range of network scenarios. In his seminal paper [2], Bianchi has laid a foundation for the modeling of CSMA/CA based WLANs, where a two-dimensional discrete time Markov chain was developed to derive per-slot statistics, such as collision and transmission probabilities. Based on these statistics, the throughput of saturated users was obtained. Several other works have followed the seminal work of [2]; for instance, the retry limit and busy medium conditions were considered in [3]. Delay performance of a single hop saturated WLAN was thoroughly studied in [4], and the average service time and jitter were derived. On the other hand, WLANs with unsaturated traffic were analyzed in [5] based on a generic queuing model, and the maximum number of concurrent voice connections that can be supported was quantified. The analytical models of these works considered a single channel WLAN with a homogeneous channel access technology among all users. Therefore, they cannot be readily applied to analyze the dynamic channel bonding or channel aggregation, where users access different channels using different channel access technologies.

The performance of dynamic channel bonding was studied based on simulations in [7]. It was shown that it can achieve an 85 percent higher throughput than a static channel bonding of 80 MHz, when secondary channels users have moderate traffic loads. The effects of hidden nodes in multi-channel WLANs were investigated in [16]. A MAC protection mechanism to combat the hidden node problem in secondary channels was proposed, and was later adopted in the IEEE 802.11ac amendment in [16]. In [17], it was shown that an 802.11ac WLAN with a single spatial stream operating over an 80 MHz wide channel can achieve a 28 percent higher throughput than an 802.11n WLAN with two spatial streams over a 40 MHz wide channel. Experimental studies in [18], [19] for 802.11n WLANs operating over a 40 MHz wide bandwidth, have shown that the channel bonding decision should consider the signal strength of links, their physical rates and the interferer load. A centralized and decentralized algorithms to dynamically select the channel center frequency and channel width were proposed in [20] and [6], respectively, to maximize the aggregate network throughput and achieve an optimal channel allocation. It is worth noting that the previous works were either based on simulations [7], [16], [17], or experimental studies from a physical layer perspective [6], [18], [19], [20], which might not be sufficient for designing efficient algorithms or giving a full insight on DCB.

A Markov chain model based on that of Bianchi's, was proposed in [21] to analyze static channel bonding in a two-channel 802.11n WLAN. It was shown that 802.11n users have lower per-slot transmission probability and conditional collision probability than single channel users. In [22], another Markov chain model was developed to study the performance of dynamic channel bonding in a two-channel WLAN. In these two works, the primary channel was exclusive for ac users and the secondary channel was exclusive for legacy users. A simplified analyical model assuming that channel idle and busy periods are exponentially distributed, was proposed in [23], to evaluate the performance of dynamic and static channel bonding, when there exists only one ac user in the primary channel. More recently, a continuous time Markov network (CTMN) model was proposed in [8], [9], to study the interactions between multiple overlapping multi-channel WLANs with asymetric channel allocations. A centralized waterfilling algorithm that provides a proportional fair channel allocation, for both the channel center frequency and channel width, was also proposed. In these works, it was shown that middle channel WLANs may starve, and random channel allocations may perform poorly in terms of throughput and fairness, compared to the proposed waterfilling algorithm. However, transmission collisions between any two or more users happen with zero-probability in this model, due to the continuous-time nature of the backoff time and absence of propagation delay. This assumption may not be true in dense networks. For instance, our previous works have shown that dynamic channel bonding degrades the overall system performance due to increased contention and collisions in the network [24], [25], [26]. In [27], an integer nonlinear optimization problem was formulated based on the CTMN of [8], [9], to maximize the system throughput. It has been shown that the maximal system throughput can be achieved when the coexisting WLANs are allocated the least overlapped channels. A CSMA based MAC, called the fine-grained spectrum sharing, was proposed in [28] to enable efficient and fair spectrum sharing among WLANs of variable widths, solving the middle-channel starvation problem. With the advancements in self-intereference cancellation techniques, a customized dynamic channel bonding (DyB) protocol with collision detection was proposed in [29]. In this protocol, a user continues to increase the channel width gradually during the transmission, as more channels become available, achieving a 20 percent throughput improvement over frame-based channel bonding.

On the other hand, few works evaluated the performance of IEEE 802.11ax. An integrated MAC-PHY system level simulation was developed in [30] to evaluate the performance of OFDMA, multi-user MIMO, non-congtiguous channel aggregation and link adaptation features of IEEE 802.11ax. Simulation results have shown that IEEE 802.11ax can achieve a higher throughput and a higher multi-channel efficiency than legacy 802.11 WLANs. The coexistence of 802.11ax users with legacy users over a single channel has been studied in [31], and a new approach was proposed such that legacy users contend for access normally, whereas 802.11ax users use AP triggered OFDMA transmissions. In this approach, EDCA parameters of the AP are tuned to achieve fair and efficient coexistence between legacy and 802.11ax users.

The analytical model we develop in this paper is fundamentally different than aforementioned works. First, with the evolution of WLANs, it is very likely that legacy users can be present in any channel, including the primary channel. Thus, our model considers a realistic network scenario where multi-channel users coexist with legacy users in potentially both the primary and secondary channels. Second, the model is extensible and applicable to any number of channels. Third, we consider collisions among users of the same channel, and among multi-channel and single channel users across different channels. Fourth, the model captures in detail channel access behaviors of different

TABLE 1
List of Notations

Notation	Description
$N^c_{mc},\ N^c_{sc}$	Number of Multi/Single channel users in Ch. c
$B^c_{mc}(j),\ B^c_{sc}(j)$	Probability that backoff counter of MC/SC user in Ch. c is j
$\beta^c_{mc}(i),\ \beta^c_{sc}(i)$	Probability that MC/SC user transmits before slot i in Ch. c
$Q^c_{mc}(i),\ Q^c_{sc}(i)$	Probability that tagged MC/SC user observes no other MC/SC user transmission before slot i in Ch. c
$\hat{Q}^c_{mc}(i),\ \hat{Q}^c_{sc}(i)$	Probability that no MC/SC user transmits before slot i in Ch. c
X^c	Number of backoff slots in a level-1 cycle in Ch. c
$E[L1^c]$	Expected level-1 cycle duration in Ch. c
P^c_s	Probability that a level-1 cycle ends in a successful transmission in Ch. c
$PS^c_{mc},\ PS^c_{sc}$	Probability that a level-1 cycle in Ch. c ends with a successful MC/SC transmission
M	Number of channels used for transmission in DCB
G_M	Channels with the same level-2 cycles in DCB
$P^{G_M}_{CB}$	Conditional probability that AC users bond group G_M
NB^{G_M}	Number of level-1 cycles of MC users in the no bonding phase
B^{G_M}	Number of level-1 cycles of MC users in the bonding phase
P^1_{busy}	Probability that the primary Ch. is busy with a transmission
P^c_{idle}	Probability that Ch. c is sensed idle for at least PIFS
PT^1_{mc}	Channel access ratio of MC users in the primary Ch.
$PT^{G_M}_{mc}$	Probability that any MC user transmits before or with any SC user in the bonding phase
P^c_b	Bonding probability in channel c in DCB
$P(SB_{mc}\|M)$	Probabilty that AC transmits successfully in a level-1 cycle in the bonding phase of M channels
$E[T_B\|M]$	Expected duration of a level-1 cycle in the bonding phase of M channels
$P_{CH}(M)$	Probability that the bonding phase involves AC transmission over M channels
$E[L2^c]$	Expected duration of a level-2 cycle in Ch. c
S^c_{mc}, S^c_{sc}	MC/SC user throughput in Ch. c

users, i.e., the full DCF operation of legacy users and multi-channel users in the primary channel, and the channel bonding access without backoff of multi-channel users in secondary channels. Fifth, the model is generic and can be applied to various multi-channel bonding schemes, including IEEE 802.11ac and IEEE 802.11ax. Our analytical results show that the selection of the primary channel can substantially affect the throughput of multi-channel users. Thus, we also propose a heuristic algorithm based on the analysis, to select the best primary channel for multi-channel users in order to maximize the achieved throughput.

4 The Analytical Model

In this section, we develop an analytical framework to study the performance of different distributed channel bonding schemes, in a single hop multi-channel WLAN, based on a two-level renewal process. In a WLAN of $C = \{1, 2, \ldots, c, \ldots, NC\}$ channels, denote N^c_{mc} and N^c_{sc} as the number of WiFi users with and without multi-channel bonding capability in channel $c, \forall c \in C$, respectively. In a single hop WLAN,

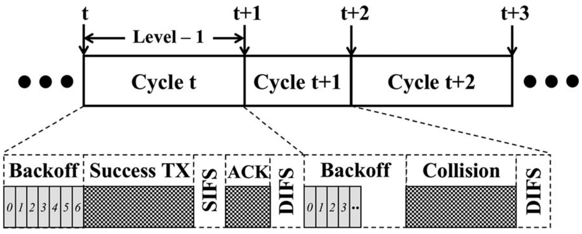

Fig. 1. Channel access process.

all users can sense the transmissions of other users, i.e., there are no hidden users. Multi-Channel (MC) users operate based on either the DCB of IEEE 802.11ac in Section 2.1, or the UCCB in Section 2.2, or CA of IEEE 802.11ax in Section 2.3. Single Channel (SC) users operate based on the legacy IEEE 802.11 DCF MAC protocol. The channel is ideal such that transmission errors only occur due to collisions among two or more simultaneous transmissions. All users are saturated, i.e., they always have data ready for transmissions, and they transmit at the highest data rate for the same duration. That is, an SC user transmits data frames of PL bytes, while an MC user transmits frames of $M * PL$ bytes when it transmits over M channels. The main notations used in this paper are tabulated in Table 1.

4.1 Backoff Distribution in a Single Channel

In this section, we derive the steady state user backoff distribution in a single channel c, which will be used in the analysis of the different bonding schemes in Sections 4.2, 4.3, and 4.4.

Generally, channel access in single channel WLANs can be modeled as an idle/busy renewal process. That is, each channel access cycle is composed of an idle period due to random backoff, followed by a busy period due to a transmission by an MC or SC user, plus a DIFS. The transmission can be either a successful transmission or a collision. This channel access cycle is referred to as a level-1 renewal process as shown in Fig. 1.

The backoff process of a typical user is modeled as a bi-dimensional Markov chain with states $\{s^c_*(t), b^c_*(t)\}$, $s^c_*(t) \in [0, R]$ and $b^c_*(t) \in [0, CW_s]$, where $s^c_*(t)$ and $b^c_*(t)$ represent the backoff stage and backoff counter of a user operating in channel c in a level-1 cycle t, respectively, $*$ is either for an MC or an SC user, R is the maximum number of retransmissions and CW_s is the maximum contention window at stage s. The discrete-time t refers to the time instant when DIFS expires after either a successful transmission or a collision, and the tth cycle starts, as shown in Fig. 1. The backoff process of the tagged user is sampled at this time instant, after a state transition from $\{s^c_*(t-1), b^c_*(t-1)\}$ to $\{s^c_*(t), b^c_*(t)\}$ has occurred. Therefore, the underlying Markov chain is in fact semi-Markov, evolving after each transmission event or every cycle. As shown in Fig. 1, at the beginning of every level-1 cycle, the system time is slotted into physical slots with index $i = 0, 1, 2 \ldots$, each of duration σ. During the idle period of a level-1 cycle t, the backoff counter of each user will be decremented every slot without interruption. The user whose backoff counter decrements to 0 first will transmit. The transmission is successful if only one user transmits, otherwise there is a collision. After a busy period and DIFS, a state transition occurs and a new level-1 cycle, the $(t+1)$th, begins.

We adopt a decoupling approximation approach [2], [32], in which all users behave statistically as the tagged user. Moreover, this approach assumes that the backoff processes as seen by the competing users at the beginning of a level-1 cycle t, are stationary, i.e., independent of the specific cycle, and independent and identically distributed. Based on these assumptions, the occurrence of level-1 cycles form a regenerative renewal process. Let $B^c_{mc}(j)$ be the steady state probability that the backoff counter of an MC user is j, i.e., $B^c_{mc}(j) = \lim_{t\to\infty} Pr\{b^c_{mc}(t) = j\}$. Define $\beta^c_{mc}(i)$ as the probability that an MC user transmits before slot i in cycle t, $\beta^c_{mc}(i) = \sum_{s=0}^{i-1} B^c_{mc}(s)$, $0 < i \le CW_{max}$, where $CW_{max} = max_{\ s\in[0,R]}\ CW_s$. Similarly for SC users, $B^c_{sc}(j) = \lim_{t\to\infty} Pr\{b^c_{sc}(t) = j\}$ and $\beta^c_{sc}(i) = \sum_{s=0}^{i-1} B^c_{sc}(s), 0 < i \le CW_{max}$. The probability that a tagged MC user observes no transmission from any other MC user before slot i in single channel c is therefore,

$$Q^c_{mc}(i) = [1 - \beta^c_{mc}(i)]^{N^c_{mc}-1}. \tag{1}$$

Similarly, the probability that a tagged SC user observes no transmission from any other SC user before slot i is,

$$Q^c_{sc}(i) = [1 - \beta^c_{sc}(i)]^{N^c_{sc}-1}. \tag{2}$$

Additionally, the probability that *no MC* user transmits before slot i, and the probability that *no SC* user transmits before slot i in channel c are given by,

$$\begin{aligned} \hat{Q}^c_{mc}(i) &= [1 - \beta^c_{mc}(i)]^{N^c_{mc}}, \\ \hat{Q}^c_{sc}(i) &= [1 - \beta^c_{sc}(i)]^{N^c_{sc}}. \end{aligned} \tag{3}$$

In general, $Q^c_{mc}(i)\hat{Q}^c_{sc}(i) - Q^c_{mc}(i+1)\hat{Q}^c_{sc}(i+1)$ is the probability that a tagged MC user observes a transmission by any other user(s) at slot i, and $Q^c_{sc}(i)\hat{Q}^c_{mc}(i) - Q^c_{sc}(i+1)\hat{Q}^c_{mc}(i+1)$ is the probability that a tagged SC user observes a transmission of another user(s) at slot i. In a similar way to [32], the state transition probabilities for MC and SC users can be therefore derived based on case analysis, as described in the Appendix, which can be found on the Computer Society Digital Library at http://doi.ieeecomputersociety.org/10.1109/TMC.2018.2857799. These transition probabilities are then used to construct the balance equations of the Markov chain, as given in the Appendix, available in the online supplemental material, which can be numerically solved using fixed point iteration, to determine the steady state probability for MC users $\Pi^c_{mc}(i,j) = \lim_{t\to\infty}\ Pr\{s^c_{mc}(t) = i, b^c_{mc}(t) = j\}$ and for SC users $\Pi^c_{sc}(i,j) = \lim_{t\to\infty} Pr\{s^c_{sc}(t) = i, b^c_{sc}(t) = j\}$. The existence and uniqueness of the steady state probability is guaranteed by the fact that the Markov chain is aperiodic (self-transitions are present), irreducible, and has a finite state space. The finiteness and irreducibility of the Markov chain imply that states are positive recurrent. Based on the steady state probabilities, the user backoff distribution is given by,

$$B^c_{mc}(j) = \sum_{s=0}^{R} \Pi^c_{mc}(s,j),\ and\ B^c_{sc}(j) = \sum_{s=0}^{R} \Pi^c_{sc}(s,j). \tag{4}$$

To find the expected duration of a level-1 cycle in channel c, denote a random variable (r.v.) X^c as the number of backoff slots in a level-1 cycle in channel c. Given k idle slots, a transmission occurs at the kth slot by either an MC user or SC user. The probability mass function (p.m.f.) of X^c is therefore,

$$Pr\{X^c = k\} = \hat{Q}^c_{mc}(k)\hat{Q}^c_{sc}(k) - \hat{Q}^c_{mc}(k+1)\hat{Q}^c_{sc}(k+1), \tag{5}$$

and the expected number of backoff slots is,

$$E[X^c] = \sum_{k=1}^{CW_{max}} k * Pr\{X^c = k\}. \tag{6}$$

The expected duration of a level-1 cycle in channel c is therefore,

$$E[L1^c] = E[X^c]\sigma + (1 - P^c_s)T_c + P^c_s T_s + DIFS, \tag{7}$$

where T_s, T_c are the duration of a successful transmission and a collision, resepectively, $T_s = T_{PL} + SIFS + T_{ACK}$ and $T_c = T_{PL}$. T_{PL} and T_{ACK} are the transmission time of a data and an ACK frame, respectively, including all headers and PHY preambles. P^c_s is the probability that a level-1 cycle ends in a successful transmission in channel c, given by $P^c_s = PS^c_{mc} + PS^c_{sc}$, where PS^c_{mc}, PS^c_{sc} are the probabilities a level-1 cycle in channel c end with a successful MC or SC transmission, respectively,

$$PS^c_{mc} = N^c_{mc} \sum_{i=0}^{CW_{max}} B^c_{mc}(i) Q^c_{mc}(i+1)\hat{Q}^c_{sc}(i+1), \tag{8}$$

and

$$PS^c_{sc} = N^c_{sc} \sum_{i=0}^{CW_{max}} B^c_{sc}(i) Q^c_{sc}(i+1)\hat{Q}^c_{mc}(i+1). \tag{9}$$

Given an MC user has a backoff counter of i at the beginning of a cycle t (probability of which is $B^c_{mc}(i)$), it will transmit successfully after i idle slots only if all other MC users and SC users are scheduled to transmit after such a slot (probability of which is $Q^c_{mc}(i+1)\hat{Q}^c_{sc}(i+1)$). The probability a level-1 cycle in channel c ends with a successful transmission by an MC user is therefore given through the total law of probability by summing over all possible values of i, times N^c_{mc}, because there are N^c_{mc} MC users. Eq. (9) is derived similarly.

4.2 IEEE 802.11n/ac Channel Bonding

In this section, we analyze the performance of the IEEE 802.11ac channel bonding MAC. We first derive the channel bonding probability in each secondary channel, and based on which, the throughput of different users in each channel is obtained.

A) Bonding Probability Analysis. MC users operating based on the 802.11ac MAC are referred to as AC users henceforth. Without loss of generality, channel 1 is the primary channel of AC users if not specified otherwise, i.e., $N^1_{mc} > 0\ and\ N^c_{mc} = 0,\ \forall c \in C - \{1\}$. In a saturated case, the impacts of the non-persistent MC user contention in secondary channels, on the steady state distribution of the backoff processes $B^1_{mc}(j)$ and $B^c_{sc}(j), \forall c$, is relatively negligible when there are many persistent contending users. That is to say, the user backoff distribution in each channel is determined by the contentions among the users of the same channel, given by (4).

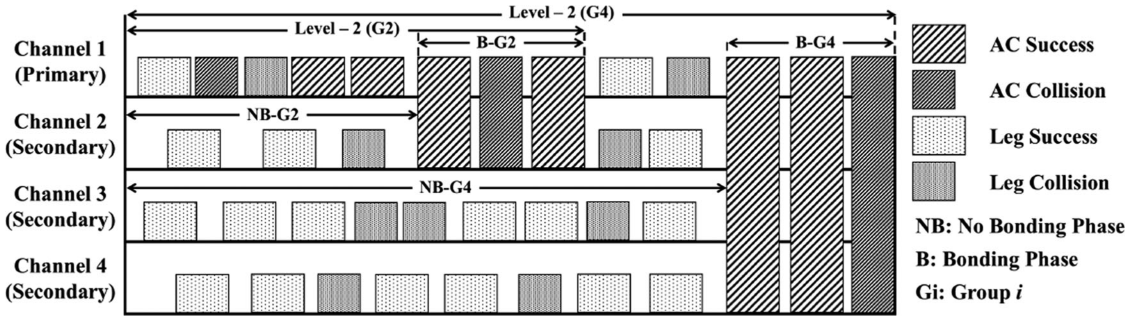

Fig. 2. An example of 2-level renewal process of channel bonding.

The occurrence of consecutive channel bonding transmissions of AC users in each secondary channel can be modeled as a level-2 renewal process, where each channel bonding cycle includes a *no bonding* phase and a *bonding* phase. In the *no bonding* phase, users launch one or multiple asynchronous transmissions in each channel, while in the *bonding* phase, transmissions in multiple channels are synchronized due to channel bonding. As shown in Fig. 2, each phase of the level-2 channel bonding cycle may involve one or multiple level-1 channel access cycles of both SC and AC users. It is worth to mention that an AC user in channel 1 may bond and transmit on a different number of channels M, where $M \in \{2, 4,\ or\ 8\}$, as specified in IEEE 802.11ac, based on the channel sensing results. Thus, the level-2 renewal cycles in each channel may be different. For instance, in the channel bonding of $M = 4$ channels, as shown in Fig. 2, channel 2 may be independently bonded with the primary channel, yet channels 3 and 4 will always be bonded together so that the level-2 channel bonding cycle in channels 3 and 4 is always the same, which can be different from that of channel 2. Similarly for $M = 8$, channels $5, 6, 7$ and 8 have the same level-2 cycle. Thus, we group the channels with the same level-2 cycles as $G_M = \{\frac{M}{2}+1, \frac{M}{2}+2, \ldots, M\}$. In other words, the bonding probability in channels which belong to the same group is the same.

Similar to the level-1 renewal process, the time between successive occurrences of level-2 cycles is independent and identically distributed. Therefore, the conditional probability that AC users successfully bond a group of secondary channels, $P_{CB}^{G_M}$, given all previous groups G_k, $\forall k < M$, $k \in \{2, 4, 8\}$, are successfully bonded, is the number of successful bonding attempts over the total number of transmissions of AC users. Define r.v. NB^{G_M} and B^{G_M} as the number of level-1 channel access cycles of AC users in the *no bonding* and *bonding* phases of the level-2 renewal process. Thus, we have

$$P_{CB}^{G_M} = \frac{E[B^{G_M}]}{E[B^{G_M}] + E[NB^{G_M}]}, \tag{10}$$

where $E[B^{G_M}]$ and $E[NB^{G_M}]$ are the expected number of level-1 channel access cycles of AC users in the *bonding* and *no bonding* phases of the level-2 channel bonding cycle, respectively.

In the *no bonding* phase, transmissions on the primary channel and the considered group of secondary channels are asynchronous single channel transmissions. Let P_{busy}^1 be the probability that the primary channel is busy with a transmission and P_{idle}^c be the probability that a secondary channel c is sensed idle for at least a PIFS during the *no bonding* phase. Given there are only AC users in the primary channel, the number of channel bonding attempts, denoted as A^{G_M}, is a geometric r.v., i.e., AC users fail in the first $A^{G_M} - 1$ attempts until a successful bonding occurs in the last attempt when all secondary channels in the group are idle, with probability $P_{busy}^1 \prod_{\forall c \in G_M} P_{idle}^c$. Therefore, the expected number of channel bonding attempts in the *no bonding* phase, given only AC users are contending in the primary channel is,

$$E[A^{G_M} | PT_{mc}^1] = \frac{1}{P_{busy}^1 \prod_{\forall c \in G_M} P_{idle}^c}, \tag{11}$$

where PT_{mc}^1 is the channel access ratio of AC users in the primary channel, which is $PT_{mc}^1 = N_{mc}^1/(N_{mc}^1 + N_{sc}^1)$ due to long time fairness. When there are also SC users in the primary channel, the expected number of AC user transmissions in the *no bonding* phase is the weighted average,

$$E[NB^{G_M}] = (E[A^{G_M} | PT_{mc}^1] - 1) PT_{mc}^1, \tag{12}$$

where the $-1 * PT_{mc}^1$ is the last successful bonding attempt, which will be included in the analysis of the *bonding* phase. In the special case when all the secondary channels in a group G_M are idle, $E[NB^{G_M}] = 0$.

In the *no bonding* phase, transmissions on different channels are asynchronous, and the probability that the primary channel is busy with a transmission, P_{busy}^1, and the probability that a secondary channel c is sensed idle for at least a PIFS, P_{idle}^c, can be readily derived based on the analysis from Section 4.1 and by applying the renewal reward theorem, as the ratio of the time that the channel is busy due to a transmission, or the ratio of the time that the channel is idle due to backoff, in a level-1 cycle, respectively,

$$P_{busy}^1 = \frac{T_{PL}}{E[L1^1]}, \tag{13}$$

and

$$P_{idle}^c = \frac{(E[X^c] + 1)\sigma}{E[L1^c]}, \tag{14}$$

where $+1$ in the numerator comes from the fact that DIFS-PIFS = 1 slot, and reflects the access priority of AC users in secondary channels.

Next, we derive $E[B^{G_M}]$, where r.v. B^{G_M} represents the number of consecutive bonded transmissions of AC users in the *bonding* phase in a group of secondary channels G_M. That is, AC users win B^{G_M} contentions with smaller backoff windows than all other SC users. After the last successful bonding attempt from the *no bonding* phase, the primary channel and the group of secondary channels are synchronized in the sense that all users decrement their backoff counters synchronously. The probability that any AC user transmits before or with any other SC user is,

$$PT_{mc}^{G_M} = \sum_{k=0}^{CW_{max}} (\hat{Q}_{mc}^1(k) - \hat{Q}_{mc}^1(k+1)) \prod_{\forall c \in G_M} \hat{Q}_{sc}^c(k)\hat{Q}_{sc}^1(k). \quad (15)$$

$\hat{Q}_{mc}^1(k) - \hat{Q}_{mc}^1(k+1)$ is the probability that an AC user transmits at slot k and $\prod_{\forall c \in G_M} \hat{Q}_{sc}^c(k)\hat{Q}_{sc}^1(k)$ is the probability that no other SC user transmits before slot k in the primary channel or the group of secondary channels G_M. The expected number of consecutive bonding success cycles is thus given by

$$E[B^{G_M}] = \sum_{b=1}^{\infty} b(PT_{mc}^{G_M})^b + PT_{mc}^1, \quad (16)$$

where the $+PT_{mc}^1$ is the last successful bonding attempt from the *no bonding* phase. Combining (12) and (16), $P_{CB}^{G_M}$ can be derived.

To successfully bond a channel c which is in group G_M, the bonding will be successful if and only if all previous groups $G_k,\ \forall k < M,\ k \in \{2,4,8\}$, are successfully bonded. For example, channel 3 in $G_4 = \{3,4\}$, can be bonded only if channel 2 in G_2, and both channels 3 and 4 in G_4 are available for channel bonding; thus, $P_b^3 = P_{CB}^{G_2} P_{CB}^{G_4}$. In general, for any channel $c > 1$, the bonding probability is

$$P_b^c = \prod P_{CB}^{G_i}, \forall i \in \{2^x; x = 1,2,\ldots,\lceil \log_2 c \rceil\}. \quad (17)$$

B) Throughput Analysis. We first derive the throughput of AC and SC users in the primary channel. In the *no bonding* phase, the contention is among AC and SC users of the primary channel only. The probability that a level-1 cycle ends with a successful AC user or SC user transmission in the *no bonding* phase are P_{mc}^1 and P_{sc}^1; as given by (8) and (9), respectively. Moreover, the expected duration of a level-1 cycle is $E[L1^1]$, given by (7).

In the bonding phase, transmissions over multiple channels are synchronized due to channel bonding, and AC users contend with both SC users in the primary and secondary channels. The probability that a level-1 cycle ends with a successful AC user transmission in the *bonding* phase, given the AC transmission is over exactly M channels is therefore,

$$P(SB_{mc}|M) = \frac{N_{mc}^1 \sum_{i=0}^{CW_{max}} B_{mc}^1(i) Q_{mc}^1(i+1) \prod_{c=1}^{M} \hat{Q}_{sc}^c(i+1)}{\sum_{k=0}^{CW_{max}} P(X_B = k|M)}, \quad (18)$$

where $P(X_B = k|M)$ is the probability that there are k idle slots at the beginning of a level-1 cycle in the *bonding* phase, given it involves exactly M channels,

$$P(X_B = k|M) = (\hat{Q}_{mc}^1(k) - \hat{Q}_{mc}^1(k+1)) \prod_{c=1}^{M} \hat{Q}_{sc}^c(k), \quad (19)$$

and thus $\sum_{k=0}^{CW_{max}} P(X_B = k|M)$ is the probability that an AC user transmits in a *bonding* phase which involves exactly M channels. The expected duration of a level-1 cycle in the bonding phase, given the bonding phase involves an AC transmission over exactly M channels is then,

$$\begin{aligned} E[T_B|M] = E[X_B|M]\sigma + P(SB_{mc}|M)T_s \\ + (1 - P(SB_{mc}|M))T_c + DIFS, \end{aligned} \quad (20)$$

where $E[X_B|M] = \sum_{k=0}^{CW_{max}} kP(X_B = k|M)$.

The *bonding* and *no bonding* phases represent level-1 cycles in the primary channel that contribute to AC user throughput, and constitute PT_{mc}^1 of the airtime in the primary channel. The complementary portion, $(1 - PT_{mc}^1)$, represents the airtime of SC users that contributes to SC user throughput in the primary channel. The expected length of the level-2 cycle in the primary channel can be therefore found as a weighted sum of the level-1 cycles in *bonding* phases involving different number of channels M, the *no bonding* phase, and SC user airtime. Denote the probability that the *bonding* phase involves AC transmission over exactly M channels as $P_{CH}(M)$,

$$P_{CH}(M) = \begin{cases} \left(\prod_{i=1}^{log_2^M} P_{CB}^{G_{2^i}}\right)\left(1 - P_{CB}^{G_{2M}}\right), & M \in \{2,4\}, \\ \prod_{i=1}^{log_2^M} P_{CB}^{G_{2^i}}, & M = 8, \end{cases} \quad (21)$$

then the expected duration of the level-2 cycle in the primary channel is,

$$\begin{aligned} E[L2^1] = PT_{mc}^1 \sum_{\forall M} P_{CH}(M) E[T_B|M] \\ + PT_{mc}^1 \left(1 - \sum_{\forall M} P_{CH}(M)\right) E[L1^1] \\ + (1 - PT_{mc}^1) E[L1^1]. \end{aligned} \quad (22)$$

During $PT_{mc}^1 \sum_{\forall M} P_{CH}(M)$ of the level-2 cycle, AC user transmission in the *bonding* phase is over exactly M channels, and the probability of a successful AC user transmission is $P(SB_{mc}|M)$ as given by (18). During $PT_{mc}^1(1 - \sum_{\forall M} P_{CH}(M))$ of the level-2 cycle, AC user transmission in the *no bonding* phase is over the primary channel only. In this case, the probability of a successful AC user transmission is $(\frac{PS_{mc}^1}{PT_{mc}^1})$, because it is now conditioned on AC user transmission. Therefore, the average throughput of AC users in the primary channel is,

$$\begin{aligned} S_{mc}^1 = \frac{PT_{mc}^1 \sum_{\forall M} P_{CH}(M) P(SB_{mc}|M) PL}{E[L2^1]} \\ + \frac{(1 - \sum_{\forall M} P_{CH}(M)) PS_{mc}^1 PL}{E[L2^1]}. \end{aligned} \quad (23)$$

On the other hand, SC users in the primary channel transmit during $(1 - PT_{mc}^1)$ of the level-2 cycle with a probability of success $(\frac{PS_{sc}^1}{1 - PT_{mc}^1})$, achieving an average throughput of S_{sc}^1,

$$S_{sc}^1 = \frac{PS_{sc}^1 PL}{E[L2^1]}. \quad (24)$$

Next, we derive the throughput of AC and SC users in each of the secondary channels. In a bonding phase of M

channels, the M channels are synchronized. Therefore, the expected duration of a level-1 cycle in each of those M secondary channels, given the *bonding* phase involves M channels, is also $E[T_B|M]$. During the *no bonding* phase and primary channel SC user airtime, the expected duration of a level-1 cycle is determined based on the contention of N^c_{sc} SC users, which is $E[L1^c]$ as given by (7). Therefore, the expected duration of the level-2 cycle in a secondary channel $c > 1$ is also found as a weighted sum of different phases,

$$\begin{aligned} E[L2^c] = {} & PT^1_{mc} \sum_{\forall M \geq 2^{\lceil \log_2^c \rceil}} P_{CH}(M) E[T_B|M] \\ & + PT^1_{mc}\left(1 - \sum_{\forall M \geq 2^{\lceil \log_2^c \rceil}} P_{CH}(M)\right) E[L1^c] \\ & + (1 - PT^1_{mc}) E[L1^c]. \end{aligned} \tag{25}$$

The average throughput of AC users in channel c, is the payload successfully delivered during $PT^1_{mc} \sum_{\forall M \geq 2^{\lceil \log_2^c \rceil}} P_{CH}(M)$ of the level-2 cycle in channel c, which is

$$S^c_{mc} = \frac{PT^1_{mc} \sum_{\forall M \geq 2^{\lceil \log_2^c \rceil}} P_{CH}(M) P(SB_{mc}|M) PL}{E[L2^c]}. \tag{26}$$

Finally, the average throughput of SC users of channel c, is the payload successfully delivered by SC users in channel c during $PT^1_{mc}(1 - \sum_{\forall M \geq 2^{\lceil \log_2^c \rceil}} P_{CH}(M))$ and $(1 - PT^1_{mc})$,

$$\begin{aligned} S^c_{sc} = {} & \frac{PT^1_{mc}(1 - \sum_{\forall M \geq 2^{\lceil \log_2^c \rceil}} P_{CH}(M)) PS^c_{sc} PL}{E[L2^c]} \\ & + \frac{(1 - PT^1_{mc}) PS^c_{sc} PL}{E[L2^c]}. \end{aligned} \tag{27}$$

4.3 Unrestricted Contiguous Channel Bonding

In this section, we extend the analysis of Section 4.2, to analyze the unrestricted contiguous channel bonding MAC, as described in Section 2.2.

MC users operating based on this MAC, referred to as UC users hereafter, select channel 1 as the primary channel if not specified otherwise, and are capable of bonding and transmitting on any number of contiguous channels, $\hat{M} \in \{2, 3, 4, \ldots, 8\}$.

In this scheme, each secondary channel has its own level-2 cycle, which may be different from other secondary channels. The analysis in Section 4.2 still holds, with some few adjustments. First, the set of channels available for bonding, M, is replaced with the set $\hat{M}$. Second, since each channel now forms its own group, we have $\hat{G}_{\hat{M}} = \hat{M}$. Third, to successfully bond channel c which is in group $\hat{G}_{\hat{M}}$, the bonding will be successful if and only if all previous groups (or channels) $\hat{G}_k,\ \forall k < \hat{M},\ k \in \{2, 3, 4, \ldots, 8\}$, are successfully bonded. Hence, for any channel $c > 1$, the bonding probability in the unrestricted continguous channel bonding MAC is,

$$\hat{P}^c_b = \prod_{\forall \hat{M} \leq c} P^{\hat{G}_{\hat{M}}}_{CB}. \tag{28}$$

Fourth, the probability that the *bonding* phase involves UC transmission over exactly $\hat{M}$ channels becomes,

$$\hat{P}_{CH}(\hat{M}) = \begin{cases} \prod_{i=2}^{\hat{M}} P^{\hat{G}_i}_{CB}\left(1 - P^{\hat{G}_{\hat{M}+1}}_{CB}\right), & \hat{M} \in \{2, 3, 4, \ldots, 7\}, \\ \prod_{i=2}^{\hat{M}} P^{\hat{G}_i}_{CB}, & \hat{M} = 8, \end{cases} \tag{29}$$

Finally, the expected duration of the level-2 cycle, the average UC and SC throughput in the primary channel can be derived in a similar way as in (22), (23) and (24), where M should be replaced by $\hat{M}$ and $P_{CH}(M)$ with $\hat{P}_{CH}(\hat{M})$. Similarly, for a secondary channel ($c > 1$), the expected duration of the level-2 cycle, the average UC and SC throughputs, can also be derived as in (25), (26) and (27), where M should be replaced by $\hat{M}$, $P_{CH}(M)$ with $\hat{P}_{CH}(\hat{M})$, and the summations are applied over $\forall \hat{M} \geq c$ instead of $\forall M \geq 2^{\lceil \log_2^c \rceil}$.

4.4 IEEE 802.11ax Channel Aggregation

In this section, we extend the analysis of Section 4.2, to analyze the performance of the IEEE 802.11ax channel aggregation MAC, as described in Section 2.3.

MC users employing channel aggregation are referred to as AX users. Similar to previous sections, we consider the case where AX users are deployed on channel 1 as the primary channel, and are capable of aggregating and transmitting on any number of channels $\tilde{M}$, $\tilde{M} \in \{2, 3, 4, \ldots, 8\}$, which may not be contiguous.

In channel aggregation, each secondary channel c is aggregated with the primary channel independently of other secondary channels, and therefore each secondary channel has its own level-2 cycle. Compared with the analysis in Section 4.2, a few modifications should be made. First, the set of channels available for bonding, M, is replaced with the set of channels available for aggregation $\tilde{M}$. Second, since each secondary channel can be independently aggregated, $\tilde{G}_{\tilde{M}} = \tilde{M}$, and furthermore,

$$\tilde{P}^c_b = P^{\tilde{G}_c}_{CB}. \tag{30}$$

Throughput analysis in primary and secondary channels can be simplified in the case of 802.11ax, due to the independency between secondary channels. Given an AX user aggregates secondary channel c, the probability that AX user transmission collides with an SC user transmission in secondary channel c, is the probability AX and SC user transmissions start at the same slot,

$$P^c_{col|B} = \sum_{k=0}^{CW_{max}} (\hat{Q}^1_{mc}(k) - \hat{Q}^1_{mc}(k+1))(\hat{Q}^c_{sc}(k) - \hat{Q}^c_{sc}(k+1)). \tag{31}$$

The total collision probability between an AX user and SC user in channel c, is found based on the total law of probability as,

$$P^c_{col} = P^c_{col|B} * \tilde{P}^c_b + 0 * (1 - \tilde{P}^c_b). \tag{32}$$

The probability that an AX user transmission is successful, is the probability the transmission is successful in the primary channel and all secondary channels,

$$PS_{ax} = PS^1_{mc} \prod_{c=1}^{8} (1 - P^c_{col}). \tag{33}$$

The throughput of AX and SC users in the primary channel are therefore,

$$\hat{S}^1_{ax} = \frac{PS_{ax}PL}{E[L1^1]}, \quad \text{and} \quad \hat{S}^1_{sc} = \frac{PS^1_{sc}PL}{E[L1^1]}. \tag{34}$$

Each secondary channel $(c > 1)$ is treated as if it is channel 2 in the analysis of 802.11ac, for which the probability a level-1 cycle ends with a successful AX user transmission $P(SB_{mc}|M = 2)$, and the expected duration of a level-1 cycle $E[T_B|M = 2]$ when secondary channel c is aggregated, are given by (18) and (20), respectively, except that the product term $\prod_{c=1}^{M} \hat{Q}^c_{sc}(*)$ reduces to $\hat{Q}^c_{sc}(*)$ only, since secondary channels are independently aggregated in AX. The expected duration of the level-2 cycle in a secondary channel $(c > 1)$, is also the weighted sum of the *bonding* phase, *no bonding* phase, and primary channel SC user airtime,

$$\begin{aligned} E[L2^c] = PT^1_{mc}\tilde{P}^c_b E[T_B|M = 2] + PT^1_{mc}(1 - \tilde{P}^c_b)E[L1^c] \\ + (1 - PT^1_{mc})E[L1^c]. \end{aligned} \tag{35}$$

The average throughput of AX users in channel c, is the payload successfully delivered during $PT^1_{mc}\tilde{P}^c_b$ of the level-2 cycle in channel c, that is

$$\hat{S}^c_{ax} = \frac{PT^1_{mc}\tilde{P}^c_b P(SB_{mc}|M = 2)PL}{E[L2^c]}. \tag{36}$$

Finally, the average throughput of SC users of channel c, is the payload successfully delivered by SC users in channel c during $PT^1_{mc}(1 - \tilde{P}^c_b)$ and $(1 - PT^1_{mc})$,

$$S^c_{sc} = \frac{PT^1_{mc}(1 - \tilde{P}^c_b)PS^c_{sc}PL}{E[L2^c]} + \frac{(1 - PT^1_{mc})PS^c_{sc}PL}{E[L2^c]}. \tag{37}$$

4.5 Homogeneous Case of MC Users

In this section, we shed the light on an interesting case where all users in the network are MC users with bonding capabilities. We show that all users will become synchronized after a while, in the sense that they freeze and decrement their backoff counters synchronously, and whoever wins the contention in its primary channel, bonds and transmits over all the available set of channels C, regardless of its primary channel or bonding scheme.

Without loss of generality, consider an MC user whose primary channel is channel 1. Since all users in channel 1 have bonding capabilities, $PT^1_{mc} = 1$. The expected number of MC user transmissions until an MC user transmits over *all* the set of available channels is $1/(P^1_{busy}\prod_{i=2}^{NC} P^c_{idle})$, given by the average of a geometric trial. During this transmission, which occupies all NC channels, the backoff counters of all other MC users are frozen, and will resume synchronously a DIFS after this transmission ends. The user whose backoff counter is the smallest among all MC users in any of the channels, will transmit over all NC channels, since PIFS $<$ DIFS. It is intuitive to see that this will be true for all successive transmissions, and regardless of the bonding scheme employed by MC users.

Based on this observation, the average throughput each MC user achieves, is the same as the average throughput it would achieve, had all MC users chosen channel 1 as the primary channel, while all secondary channels are left free,

$$S_H = NC\frac{PS^*_H PL}{E[L1^*]}, \tag{38}$$

where PS^*_H is the probability a level-1 cycle in channel 1 ends with a successful transmission for an MC user, when there exist $N_H = \sum_{c=1}^{NC} N^c_{mc}$ total MC users in channel 1,

$$PS^*_H = \sum_{i=0}^{CW_{max}} B^1_{mc}(i)Q^1_{mc}(i + 1), \tag{39}$$

and $E[L1^*] = E[L1^c]$, given by (7), with $P^c_s = N_H PS^*_H$.

5 Primary Channel Selection

MC users contend mainly over the primary channel using DCF, and only sense secondary channels for a PIFS to gain multi-channel access. Selection of the primary channel therefore plays a critical role in achieving a high throughput performance of MC users. In this section, we propose a primary channel selection algorithm for multi-channel WLANs, so that MC users select the best primary channel that maximizes the throughput they achieve.

First, we define an objective function $J(c)$ to characterize the average total throughput of MC users when channel c is selected as the primary channel, i.e.,

$$\begin{aligned} J(c) = Pr\{upward|c\}\left(\sum_{\forall k \in L(c,up)} S^k_{mc}\right) \\ + Pr\{downward|c\}\left(\sum_{\forall k \in L(c,down)} S^k_{mc}\right), \end{aligned} \tag{40}$$

where $L(c, up)$, $L(c, down)$ are the set of channels accessible by an MC user in the upward and downward directions, respectively, when it selects channel c as the primary channel, $Pr\{upward|c\}$ and $Pr\{downward|c\}$ are the bonding direction likelihoods, when channel c is selected as a primary channel, $Pr\{upward|c\} + Pr\{downward|c\} = 1$. If an MC user selects channel 3 as a primary channel in DCB for instance, $L(3, up) = \{3, 2\}$ and $L(3, down) = \{3, 4, 5, 6\}$, because the number of channels used for transmission must be powers of 2 in DCB. In UCCB, $L(3, up) = \{3, 2, 1\}$ and $L(3, down) = \{3, 4, 5, 6, 7, 8\}$. In CA, however, $L(c, up) = L(c, down) = C$, $\forall c$ since there is no restriction on the contiguity or number of channels. The likelihood of upward bonding for channel c, $Pr\{upward|c\}$, depends on the contention level of the most adjacent secondary channel in the upward direction, i.e., $(c - 1)$, and in the downward direction, i.e., $(c + 1)$. Intuitively, upward bonding will be favored over downward bonding when channel $(c - 1)$ is less congested compared to channel $(c + 1)$, i.e., $N^{c-1}_{sc} < N^{c+1}_{sc}$. Hence, $Pr\{upward|c\}$ can be estimated as,

$$Pr\{upward|c\} = \begin{cases} \frac{N^{c+1}_{sc}}{N^{c+1}_{sc}+N^{c-1}_{sc}}, & N^{c+1}_{sc} + N^{c-1}_{sc} > 0, \\ \frac{1}{2}, & N^{c+1}_{sc} + N^{c-1}_{sc} = 0. \end{cases} \tag{41}$$

Notice that if c is a boundary channel, i.e., $c = 1$ or $c = 8$, the bonding direction will certainly be downward for $c = 1$ ($Pr\{downward|1\} = 1$), and upward for $c = 8$ ($Pr\{upward|8\} = 1$). Similarly, if the most adjacent secondary channel in one

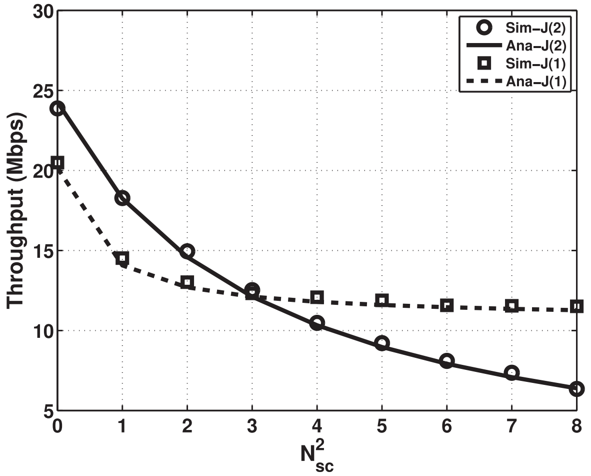

Fig. 3. J function.

direction is free, the bonding will be in its direction with probability 1. In the special case when both $(c-1)$ and $(c+1)$ are free, the direction of bonding is uniformly chosen.

To attain the maximum throughput, MC users should select a primary channel c which maximizes J, i.e., $c = max_{\ c \in C}\ J(c)$. The optimization problem in (40) is an integer optimization problem; however, the optimal channel selection can be found by methods such as branch and bound. Fig. 3 plots the J function in a two channel case. We have an IEEE 802.11ac WLAN with 4 users, that would either select channel 1 (dashed curve) or 2 (continuous curve) as a primary channel. Channel 1 is occupied with $N^1_{sc} = 3$ SC users, while the number of SC users in channel 2, N^2_{sc}, varies. It can be seen that AC users attain a higher throughput by selecting channel 2 as a primary channel, so long as channel 2 has a smaller number of SC users compared to channel 1, i.e., when $N^2_{sc} < N^1_{sc}$. Motivated by this observation, we propose a heuristic algorithm for primary channel selection in multi-channel WLANs, in which MC users select the best primary channel by maximizing a utility function, $\mathcal{U}(c)$, that reflects the total throughput achieved, but is only a function of the number of MC and SC users in the network. First, the saturation throughput of MC users in a primary channel c is estimated by the number of MC users, to the total number of users in the primary channel, i.e., $\frac{N^c_{mc}}{N^c_{mc}+N^c_{sc}}$. Furthermore, the saturation throughput of MC users in the downward secondary channel $(c+1)$, is estimated by $\frac{N^c_{mc}}{N^c_{mc}+N^c_{sc}} \frac{N^c_{mc}}{N^c_{mc}+N^{c+1}_{sc}}$, where the latter fraction estimates the bonding probability in channel $(c+1)$. Similar estimations are performed for the rest of the secondary channels in both directions. In general, for a given N_{mc}, N^c_{sc}, M, $\mathcal{M}_M$, and a set of channels, H^c_M, available for bonding, which depends on the channel bonding scheme and bonding direction, the utility function can be given by,

$$\mathcal{U} = \left(\frac{N_{mc}}{N_{mc}+N^c_{sc}}\right)\left(1 \ + \sum_M |H^c_M| \prod_{j=1}^{\mathcal{M}_M} \left(\frac{N_{mc}}{N_{mc}+\sum_{i \in H^c_{M_j}} N^i_{sc}}\right)\right), \tag{42}$$

where M_j is the jth element in the set M. In DCB, $\mathcal{M}_M = \log_2^M$, H^c_M is set to $D^c_M = \{\frac{M}{2}+c, \frac{M}{2}+c+1, \ldots, M+c-1\}$, $\forall M, c, (M+c-1) \le 8$, in the downward direction, and to $U^c_M = \{c-\frac{M}{2}, c-\frac{M}{2}-1, \ldots, c-M+1\}$, $\forall M, c, (c-M+1) > 0$, in the upward direction. In UCCB however, M is again replaced with $\hat{M}$, and accordingly, $\mathcal{M}_{\hat{M}} = \hat{M}-1$, $H^c_{\hat{M}}$ is set to $D^c_{\hat{M}} = \{\hat{M}+c-1\}$, $\forall \hat{M}, c, (\hat{M}+c-1) \le 8$, in the downward direction, and to $U^c_{\hat{M}} = \{c-\hat{M}+1\}$, $\forall \hat{M}, c$, $(c-\hat{M}+1) > 0$, in the upward direction. Based on (42) and the aforementioned channel set characterization, the implementation of our proposed primary channel selection algorithm is outlined in Algorithm 1. While this selection scheme is valid for AC and UC users, it suffices for AX users to choose the channel which has the least contentions, without considering secondary channels, i.e., $c = argmin_{\ \forall c \in [1,8]}\ N^c_{sc}$ in the case of CA.

TABLE 2
Simulation Parameters

Parameter	Value
$PL\ (with\ headers)$	576 $bytes$
$T_{PL}(with\ headers)$	108 μs
σ	9 μs
$DIFS$	34 μs
$PIFS$	25 μs
$SIFS$	16 μs
T_{ACK}	28 μs
CW_0	15
CW_{max}	255
R	7

Algorithm 1. Primary Channel Selection

Input: N_{mc}, N^c_{sc}, $\forall c \in [1, 8]$
Output: c
1: **Initialize:** $M,\ \mathcal{M}_M, D^c_M, U^c_M$ according to the channel bonding scheme and direction
2: **for** $c \in \{1, 2, 3, \ldots, 8\}$ **do**
3: update $\mathcal{U}_d(c)$ using (42) and setting H^c_M to D^c_M
4: update $\mathcal{U}_u(c)$ using (42) and setting H^c_M to U^c_M
5: $\mathcal{U}(c) = P\{downward|c\}\mathcal{U}_d(c) + P\{upward|c\}\mathcal{U}_u(c)$
6: **end**
7: $c = argmax_{\ \forall c \in [1,8]}\mathcal{U}(c)$

6 Performance Evaluation

We implemented the DCB, UCCB and the CA multi-channel schemes in an event driven network simulator (NS-3) for performance evaluation. We set up a single hop multi-channel WLAN with N^1_{mc} MC users on channel 1, and N^c_{sc} SC users on channel $c, \forall c \in C$. All users transmit saturated uplink traffic at a rate of 54 Mbps to the AP with which they are associated. The main parameters are listed in Table 2.

We first study the bonding probability and throughput performance of the different channel bonding schemes, in a four-channel setting, with $N^1_{mc} = 5$, $N^1_{sc} = N^3_{sc} = 0$, and a variable number of SC users in channels 2 and 4, $N^2_{sc} = N^4_{sc}$, in Figs. 4 and 5. For the DCB, it can be observed in Fig. 4a that the bonding probability decreases as the number of SC users in secondary channels increase, and the throughput of AC users decreases accordingly in Fig. 5a. In this case, the bonding probability in channels 3 and 4, P^3_B and P^4_B, is the same, and is much less than that of channel 2, P^2_B. This is because secondary channel 2 can be bonded alone according to DCB,

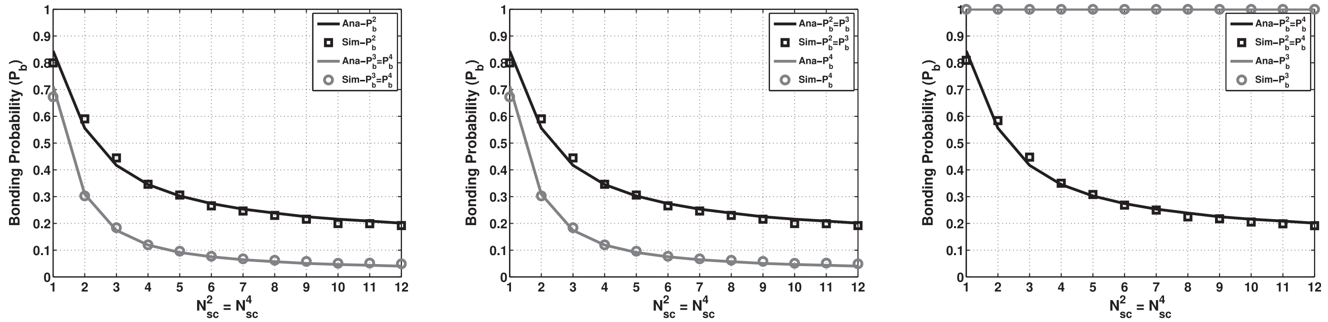

(a) DCB (b) UCCB (c) CA

Fig. 4. Bonding probability under different bonding schemes $(N_{mc}^1 = 5,\ N_{sc}^1 = N_{sc}^3 = 0)$.

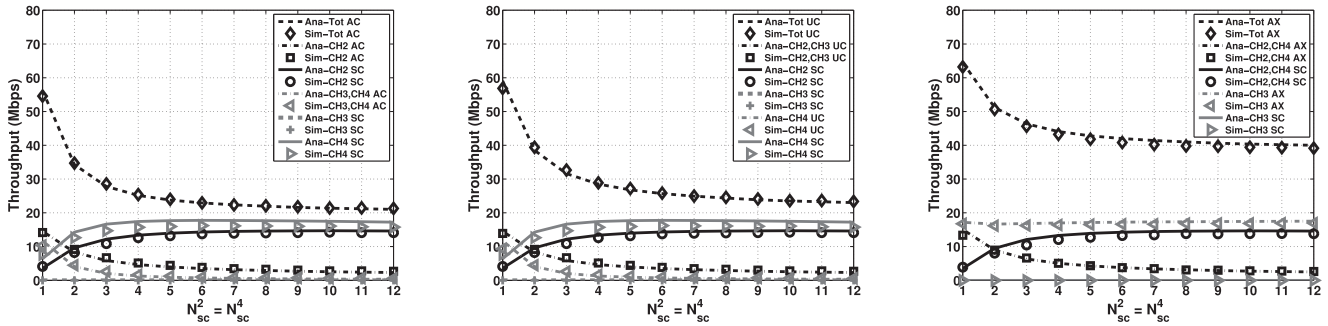

(a) DCB (b) UCCB (c) CA

Fig. 5. Throughput under different bonding schemes $(N_{mc}^1 = 5,\ N_{sc}^1 = N_{sc}^3 = 0)$.

or channels 2, 3 and 4 are bonded altogether if they are all idle, which is a less probable event. The throughput gain-loss relationship between AC and SC users is illustrated in Fig. 5a. A higher throughput of SC users can be achieved with more SC users in channels 2 and 4, yet less likely an AC user can bond secondary channels for its transmissions. AC users achieve a higher throughput in channel 2 compared to that achieved in channels 3 and 4, and in turn, SC users of channel 2 achieve lower throughput compared to that achieved by SC users in channel 4. This is also because of the sequential bonding structure of DCB. The small gap between simulation and analysis is due to the impacts of MC user contention in secondary channels on the steady state distribution of users' backoff processes, which have been ignored in the analysis.

The bonding probability and throughput performance of UCCB and CA are shown in Figs. 4b and 4c and Figs. 5b and 5c. The overall gain-loss relationship between MC and SC users is the same, with some minor differences. Unlike DCB, $P_B^2 = P_B^3$ in the case of UCCB, and P_B^4 is much less. This is because channel 3 is free and is always bonded whenever channel 2 is bonded, whereas channel 4 is bonded only if all channels 2, 3 and 4 are idle. This is also reflected in the throughput breakdown in Fig. 5b. For CA, every secondary channel is independently aggregated. Therefore, $P_B^2 = P_B^4$ in Fig. 4c, and $S_{ac}^2 = S_{ac}^4,\ S_{sc}^2 = S_{sc}^4$ in Fig. 5c, because channels 2 and 4 have an equal number of SC users. On the other hand, P_B^3 is always 1, and S_{ac}^3 is constant in channel 3. This is because channel 3 is free and therefore is always aggregated with the primary channel. Total MC user throughput under different bonding schemes is compared in Fig. 6. It can be seen that CA achieves the highest throughput, followed by UCCB and lastly DCB. It is interesting to observe that the throughput performance of DCB and UCCB is comparable, although the rule for accessing channel 3, which is free, is different. CA on the other hand, is more efficient in exploiting this free channel, and hence achieving the 18 Mbps gap. Fig. 7 illustrates another comparison between different bonding schemes when all secondary channels are occupied with SC users, $N_{sc}^2 = N_{sc}^3 = N_{sc}^4$, and 8 MC users are deployed in channel 1. It can also be seen that the performance of DCB and UCCB is comparable, yet CA outperforms them both and achieves a $5 \sim 10$ Mbps higher throughput.

In Figs. 8 and 9, we study the effects of the minimum contention window and payload size on DCB in a four-channel WLAN, with $N_{mc}^1 = 8$ and $N_{sc}^2 = N_{sc}^3 = N_{sc}^4 = 4$. It is interesting to observe that AC users achieve a higher throughput as the minimum contention window CW_0 increases in Fig. 8. This is because with a larger contention window, idle periods in secondary channels are longer, and therefore AC users are more likely to find secondary channels idle. In Fig. 9, it is

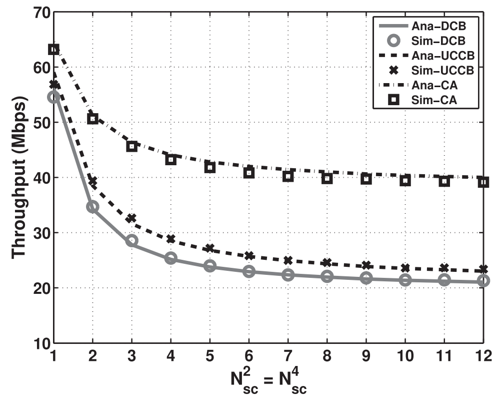

Fig. 6. Bonding schemes throughput comparison $(N_{mc}^1 = 5,\ N_{sc}^1 = N_{sc}^3 = 0)$.

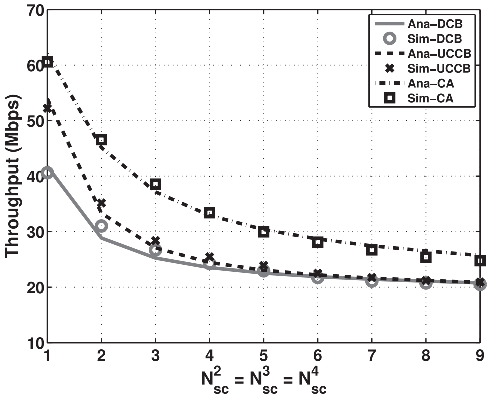

Fig. 7. Bonding schemes throughput comparison ($N^1_{mc} = 8$, $N^1_{sc} = 0$).

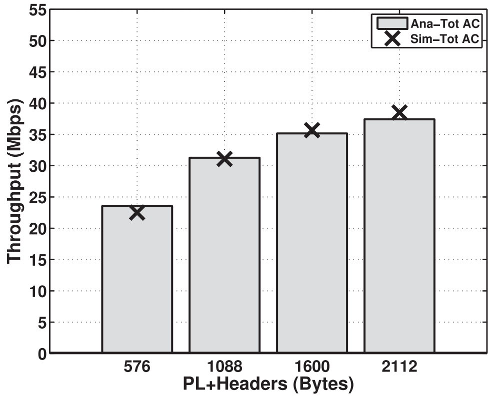

Fig. 9. Throughput comparison under different payload sizes (DCB) ($N^1_{mc} = 10$, $N^1_{sc} = 0$).

shown that AC user throughput increases as payload size increases. This is expected because in CSMA/CA, the backoff overhead becomes marginal as transmission time increases. Simulation results also validate the accuracy of the analysis.

Fig. 10 shows the throughput performance of a homogeneous WLAN in a four-channel setting, when all users in the network are MC users. $N^c_{mc},\ c \in [1,4]$ users with bonding capabilities are deployed on channels $\{1,2,3,4\}$, and are referred to hereafter as WLANs $\{A,B,C,D\}$, respectively. It can be seen that the total throughput of the system is broken down proportionally according to the number of users in each WLAN. In another experiment, $N_H = \sum_1^4 N^c_{mc}$ users with bonding capabilities are deployed on channel 1 as the primary channel, forming WLAN E, and all secondary channels are left free. It can be observed that this WLAN achieves the same total throughput achieved by WLANs $\{A,B,C,D\}$, although they have different primary channel selections, verifying our logical reasoning.

The performance of the primary channel selection algorithm for each of the bonding schemes, is evaluated in Fig. 11 under random presence of SC users over channels 1 through 8. Figs. 11a and 11b represent a case where some channels are free and others are relatively lightly loaded, while Figs. 11c and 11d represent a case where all the channels are relatively densely loaded with SC users. In each of these figures, a multi-channel WLAN of 5 users select the primary channel based on either the optimal selection as in (40), or the proposed heuristic selection, or a random selection, or fixed selection of channel 1. In the case of the optimal and heuristic selections, the numbers above the bars represent the selected channel index according to the given selection scheme. In the case of random selection, the average throughput achieved is calculated. It can be seen that the heuristic algorithm is sub-optimal compared to the exhaustive optimal selection, yet it always outperforms random selection and fixed selection. It can also be seen that the total MC user throughput in CA is always higher than that of UCCB or DCB, and that the throughput performance of UCCB is comparable to that of DCB. More importantly, it can be observed that the throughput performance of CA is nearly double that of UCCB or DCB when channels are relatively dense (Figs. 11c and 11d), which suggests that CA is less friendly when it comes to the coexistence with SC users, compared to contiguous channel bonding schemes, DCB and UCCB.

7 Conclusion

In this paper, we have developed an analytical model based on renewal theory to study the performance of multi-channel MAC protocols in IEEE 802.11 WLANs, with coexisting legacy single channel users. It is found that the dynamic channel bonding of 802.11ac can boost the throughput of multi-channel users, while providing a friendly coexistence with single channel users in densely loaded channels. However, it is sometimes incapable of exploiting under-utilized secondary channels due to the sequential contiguous bonding restriction. On the other hand, channel aggregation of 802.11ax provides a more flexible means of utilizing secondary channels, although it is less friendly in terms of coexistence with single channel users. Based on the analysis, an algorithm has been developed for multi-channel users to

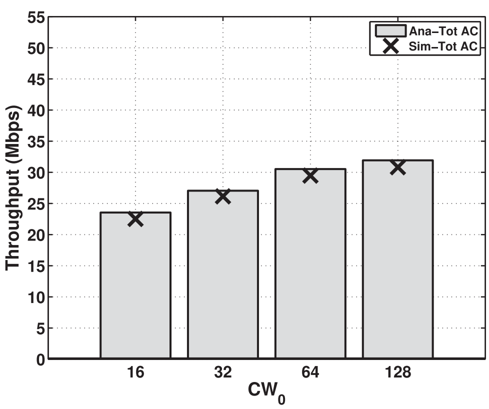

Fig. 8. Throughput comparison under different Contention window sizes (DCB) ($N^1_{mc} = 10$, $N^1_{sc} = 0$).

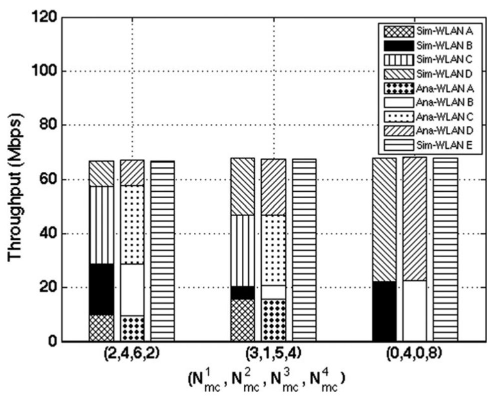

Fig. 10. Throughput when all users are MC users.

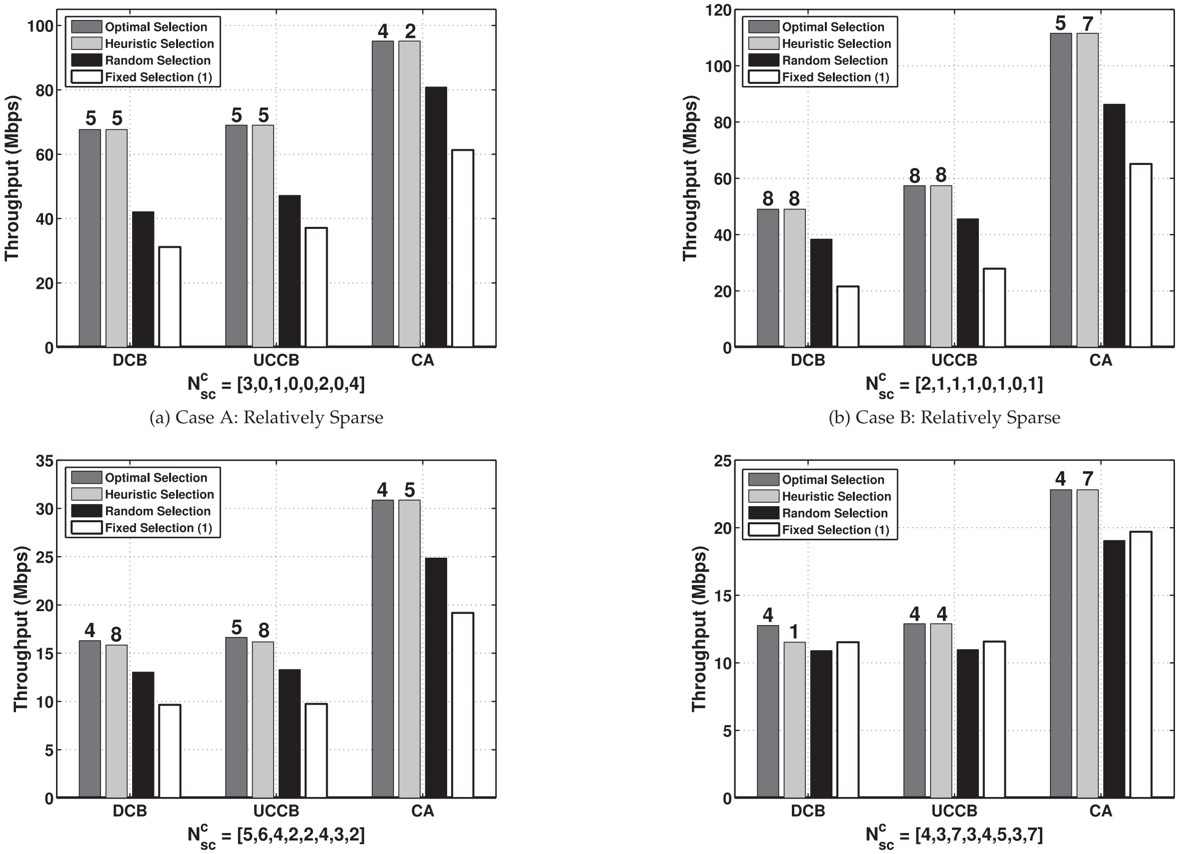

(a) Case A: Relatively Sparse

(b) Case B: Relatively Sparse

(c) Case C: Relatively Dense

(d) Case D: Relatively Dense

Fig. 11. Primary channel selection ($N_{mc} = 5$).

select the best primary channel in order to attain the maximum throughput. In our future work, we will extend our analytical framework to analyze the coexistence of multi-channel WLANs with legacy single channel users in multi-hop, multi-cell HetNets, under a wireless fading channel.

Acknowledgments

This work was supported in part by NSF grants ECCS-1554576, ECCS-1610874, CNS-1717454, CNS-1731424, CNS-1702850, CNS-1646607, ECCS-1547201, and US MURI.

References

[1] Cisco, "Cisco Visual Networking Index: Global Mobile Data Traffic Forecast Update, 2016-2021," Feb. 2017, https://www.cisco.com/c/en/us/solutions/collateral/service-provider/visual-networking-index-vni/vni-forecast-qa.html

[2] G. Bianchi, "Performance analysis of the IEEE 802.11 distributed coordination function," *IEEE J. Sel. Areas Commun.*, vol. 18, no. 3, pp. 535–547, Mar. 2000.

[3] E. Ziouva and T. Antonakopoulos, "CSMA/CA performance under high traffic conditions: Throughput and delay analysis," *Comput. Commun.*, vol. 25, no. 3, pp. 313–321, Feb. 2002.

[4] M. M. Carvalho and J. Garcia-Luna-Aceves, "Delay analysis of IEEE 802.11 in single-hop networks," in *Proc. 11th IEEE Int. Conf. Netw. Protocols*, Nov. 2003, pp. 146–155.

[5] L. X. Cai, X. Shen, J. W. Mark, L. Cai, and Y. Xiao, "Voice capacity analysis of WLAN with unbalanced traffic," *IEEE Trans. Veh. Technol.*, vol. 55, no. 3, pp. 752–761, May 2006.

[6] J. Herzen, R. Merz, and P. Thiran, "Distributed spectrum assignment for home WLANs," in *Proc. IEEE INFOCOM*, Apr. 2013, pp. 1573–1581.

[7] M. Park, "IEEE 802.11ac: Dynamic bandwidth channel access," in *Proc. IEEE Int. Conf. Commun.*, Jun. 2011, pp. 1–5.

[8] B. Bellalta, A. Checco, A. Zocca, and J. Barcelo, "On the interactions between multiple overlapping WLANs using channel bonding," *IEEE Trans. Veh. Technol.*, vol. 65, no. 2, pp. 796–812, Feb. 2016.

[9] A. Faridi, B. Bellalta, and A. Checco, "Analysis of dynamic channel bonding in dense networks of WLANs," *IEEE Trans. Mobile Comput.*, vol. 16, no. 8, pp. 2118–2131, Aug. 2017.

[10] "IEEE Standard for Information Technology—Local and Metropolitan Area Networks—Specific Requirements—Part 11: Wireless LAN Medium Access Control (MAC) and Physical Layer (PHY) Specifications Amendment 5: Enhancements for Higher Throughput," *IEEE Std 802.11n-2009 (Amendment to IEEE Std 802.11-2007)*, pp. 1–565, Oct. 2009, doi: 10.1109/IEEESTD.2009.5307322.

[11] "IEEE Std 802.11ac(TM)-2013 (Amendment to IEEE Std 802.11-2012)," *IEEE Standard for Information Technology—Local and Metropolitan Area Networks—Specific Requirements—Part 11: Wireless LAN Medium Access Control (MAC) and Physical Layer (PHY) Specifications–Amendment 4: Enhancements for Very High Throughput for Operation in Bands below 6 GHz.*, pp. 1– 425. Dec. 2013.

[12] "IEEE Std 802.11-2007 (Revision of IEEE Std 802.11-1999)," *IEEE 802.11 Standard for Wireless LAN Medium Access Control (MAC) and Physical Layer (PHY) specifications*, pp. 1–1238, Jun. 2007.

[13] X. Ling, Y. Cheng, J. W. Mark, and X. Shen, "A renewal theory based analytical model for the contention access period of IEEE 802.15.4 MAC," *IEEE Trans. Wireless Commun.*, vol. 7, no. 6, pp. 2340–2349, Jun. 2008.

[14] IEEE P802.11-TASK GROUP AX. Jun. 22, 2017. [Online]. Available: http://www.ieee802.org/11/Reports/tgax_update.htm

[15] B. Bellalta, "IEEE 802.11ax: High-efficiency WLANS," *IEEE Wireless Commun.*, vol. 23, no. 1, pp. 38–46, Feb. 2016.

[16] M. X. Gong, B. Hart, L. Xia, and R. Want, "Channel bounding and MAC protection mechanisms for 802.11ac," in *Proc. IEEE Global Telecommun. Conf.*, Dec. 2011, pp. 1–5.

[17] E. H. Ong, J. Kneckt, O. Alanen, Z. Chang, T. Huovinen, and T. Nihtilä, "IEEE 802.11ac: Enhancements for very high throughput WLANs," in *Proc. IEEE 22nd Int. Symp. Pers. Indoor Mobile Radio Commun.*, Sep. 2011, pp. 849–853.

[18] L. Deek, E. Garcia-Villegas , E. Belding, S.-J. Lee, and K. Almeroth, "Intelligent channel bonding in 802.11n WLANs," *IEEE Trans. Mobile Comput.*, vol. 13, no. 6, pp. 1242–1255, Jun. 2014.

[19] L. Deek, E. Villegas, E. Belding, S. Lee, and K. Almeroth, "The impact of channel bonding on 802.11n network management," in *Proc. 7th ACM Conf. Emerging Netw. Experiments Technol.*, Dec. 2011, Art. no. 11.

[20] M. Y. Arslan, K. Pelechrinis, I. Broustis, S. V. Krishnamurthy, S. Addepalli, and K. Papagiannaki, "Auto-configuration of 802.11n WLANs," in *Proc. 6th ACM Int. Conf.*, Jul. 2010, Art. no. 27.

[21] S. Pollin and A. Bahai, "Performance analysis of double-channel 802.11n contending with single-channel 802.11," in *Proc. IEEE Int. Conf. Commun.*, Jun. 2009, pp. 1–6.

[22] S. V. S V, S. S, and V. Ramaiyan, "Performance analysis of an IEEE 802.11ac WLAN with dynamic bandwidth channel access," in *Proc. 22nd Nat. Conf. Commun.*, Mar. 2016, pp. 1–6.

[23] B. Bellalta, A. Faridi, J. Barcelo, A. Checco, and P. Chatzimisios, "Channel bonding in short-range WLANs," in *Proc. 20th Eur. Wireless Conf.*, May 2014, pp. 1–7.

[24] M. Han, S. Khairy, L. X. Cai, and Y. Cheng, "Performance analysis of opportunistic channel bonding in multi-channel WLANs," in *Proc. IEEE Global Telecommun. Conf.*, Dec. 2016, pp. 1–6.

[25] S. Khairy, M. Han, L. X. Cai, Y. Cheng, and Z. Han, "Enabling efficient multi-channel bonding for IEEE 802.11ac WLANs," in *Proc. IEEE Int. Conf. Commun.*, May 2017, pp. 1–6.

[26] M. Han, S. Khairy, L. X. Cai, and Y. Cheng, "Performance analysis of video services over WLANs with multi-channel bonding," in *Proc. IEEE 86th Veh. Technol. Conf.*, Sep. 2017, pp. 1–5.

[27] C. Kai, Y. Liang, T. Huang, and X. Chen, "To bond or not to bond: An optimal channel allocation algorithm for flexible dynamic channel bonding in WLANs," *2017 IEEE 86th Vehicular Technol. Conf. (VTC-Fall)*, pp. 1–6, Sept. 2017.

[28] S. Han, X. Zhang, and K. G. Shin, "Fair and efficient coexistence of heterogeneous channel widths in next-generation Wireless LANs," *IEEE Trans. Mobile Comput.*, vol. 15, no. 11, pp. 2749–2761, Nov. 2016.

[29] P. Huang, X. Yang, and L. Xiao, "Dynamic channel bonding: Enabling flexible spectrum aggregation," *IEEE Trans. Mobile Comput.*, vol. 15, no. 12, pp. 3042–3056, Dec. 2016.

[30] W. Lin, B. Li, M. Yang, Q. Qu, Z. Yan, X. Zuo, and B. Yang, "Integrated link-system level simulation platform for the next generation WLAN-IEEE 802.11ax," in *Proc. IEEE Global Commun. Conf.*, Dec. 2016, pp. 1–7.

[31] E. Khorov, V. Loginov, and A. Lyakhov, "Several EDCA parameter sets for improving channel access in IEEE 802.11ax networks," in *Proc. Int. Symp. Wireless Commun. Syst.*, Sep. 2016, pp. 419–423.

[32] I. Tinnirello and G. Bianchi, "Rethinking the IEEE 802.11e EDCA performance modeling methodology," *IEEE/ACM Trans. Netw.*, vol. 18, no. 2, pp. 540–553, Apr. 2010.

Sami Khairy received the BS degree in computer engineering from the University of Jordan, Amman, Jordan, in 2014 and the MS degree in electrical engineering from the Illinois Institute of Technology, Chicago, IL, in 2016. He is currently working towards the PhD degree in electrical engineering at the Illinois Institute of Technology. His research interests include network performance analysis and protocol design for wireless communication networks, resource allocation, green communications, signal processing, and pattern recognition. He received a Fulbright Predoctoral Scholarship from the Jordanian-American Commission for Educational Exchange (JACEE) and the US Department of State in 2015. He is a student member of the IEEE.

Mengqi Han received the BS degree in electrical engineering from the Nanjing University of Science and Technology, Nanjing, China, in 2013 and the MS degree in electrical engineering from the Illinois Institute of Technology, Chicago, IL, in 2015. She is now working toward the PhD degree in electrical engineering at the Illinois Institute of Technology. Her research interests include performance analysis of MAC protocols and protocol design for Wi-Fi and Unlicensed-LTE. She is a student member of the IEEE.

Lin X. Cai received the MASc and PhD degrees in electrical and computer engineering from the University of Waterloo, Waterloo, Canada, in 2005 and 2010, respectively. She was a postdoctoral research fellow in the Electrical Engineering Department at Princeton University, in 2011 before she joined the Huawei US Wireless R&D Center as a senior engineer, in 2012. She has been an assistant professor with the Department of Electrical and Computer Engineering, Illinois Institute of Technology, Chicago, Illinois, since August 2014. Her research interests include green communication and networking, broadband multimedia services, and radio resource and mobility management. She received a postdoctoral fellowship award from the Natural Sciences and Engineering Research Council of Canada (NSERC), in 2010, a best paper award from the IEEE Globecom 2011, and an NSF Career Award in 2016. She is an associate editor for the *IEEE Network Magazine*, and has been a co-chair for IEEE conferences. She is a member of the IEEE.

Yu Cheng received the BE and ME degrees in electrical engineering from Tsinghua University, Beijing, China, in 1995 and 1998, respectively, and the PhD degree in electrical and computer engineering from the University of Waterloo, Waterloo, Ontario, Canada, in 2003. From September 2004 to July 2006, he was a postdoctoral research fellow with the Department of Electrical and Computer Engineering, University of Toronto, Ontario, Canada. Since August 2006, he has been with the Department of Electrical and Computer Engineering, Illinois Institute of Technology, Chicago, Illinois, and he is now an associate professor. His research interests include next-generation Internet architectures and management, wireless network performance analysis, network security, and wireless/wireline interworking. He received a postdoctoral fellowship award from the Natural Sciences and Engineering Research Council of Canada (NSERC), in 2004, and a Best Paper Award from the conferences QShine 2007 and ICC 2011, and the Best Paper Runner-Up Award from ACM MobiHoc 2014. He received the National Science Foundation (NSF) Career Award in 2011 and IIT Sigma Xi Research Award in the junior faculty division in 2013. He has served as a co-chair of IEEE conferences. He is an associated editor for the *IEEE Transactions on Vehicular Technology*, and the New Books & Multimedia Column Editor for the *IEEE Network*. He is an IEEE senior member and an IEEE ComSoc distinguished lecturer.

Zhu Han received the BS degree in electronic engineering from Tsinghua University, in 1997, and the MS and PhD degrees in electrical and computer engineering from the University of Maryland, College Park, in 1999 and 2003, respectively. From 2000 to 2002, he was an R&D engineer of JDSU, Germantown, Maryland. From 2003 to 2006, he was a research associate with the University of Maryland. From 2006 to 2008, he was an assistant professor with Boise State University, Idaho. Currently, he is a professor with the Electrical and Computer Engineering Department as well as in the Computer Science Department, University of Houston, Texas. His research interests include wireless resource allocation and management, wireless communications and networking, game theory, big data analysis, security, and smart grid. He received an NSF Career Award in 2010, the Fred W. Ellersick Prize of the IEEE Communication Society in 2011, the EURASIP Best Paper Award for the *Journal on Advances in Signal Processing* in 2015, IEEE Leonard G. Abraham Prize in the field of Communications Systems (best paper award in IEEE JSAC) in 2016, and several best paper awards in IEEE conferences. He has been an IEEE fellow since 2014 and is currently an IEEE Communications Society distinguished lecturer.